Thermotropic Behavior of Lipophilic Derivatized [60]Fullerenes Studied by Deuterium NMR, X-ray Diffraction, and Microcalorimetry

Michael Hetzer,[†] Thomas Gutberlet,[‡] Michael F. Brown,[§] Xavier Camps,[||] Otto Vostrowsky,[||] Hubert Schönberger,[||] Andreas Hirsch,[||] and Thomas M. Bayerl*,[†]

Physikalisches Institut EP-5, Universität Würzburg, D-97074 Würzburg, Germany, Institut für Organische Chemie, Universität Erlangen-Nürnberg, D-91054 Erlangen, Germany, Department of Chemistry, University of Arizona, Tucson, Arizona 85721, and Physikalisches Institut, Universität Leipzig, D-04103 Leipzig, Germany

Received: August 20, 1998; In Final Form: November 12, 1998

The dynamics, structure, and thermotropic behavior of a new class of lipophilic [60]fullerene (C_{60}) derivatives, so-called lipo-fullerenes, have been studied by differential scanning calorimetry (DSC), deuterium nuclear magnetic resonance (^{2}H NMR), and X-ray scattering. The lipo-fullerene studied consists of six pairs of perdeuterated C_{18} alkyl chains as substituents of six covalently attached methylene groups in octahedral sites. The symmetry of this highly symmetrical hexamethanofullerene is T_h. We find drastic changes of the molecular arrangement of the lipo-fullerenes induced by temperature. Heating the sample from 20 to 70 °C causes it to undergo two major structural transitions. At 55 °C we observe an exothermic transition from a low-temperature, hard sphere-like packing state of the molecules, with separation distances (6.1 nm) slightly above the maximum diameter of the molecules, to a condensed one. This latter state involves partial intercalation (interdigitation) of the alkyl chains belonging to adjacent molecules and is preceded by partial melting of the chains to accommodate sterically for the (exothermic) interdigitation. The latter allows denser packing with an average separation distance of 4.8 nm. At a temperature of 64 °C, an endothermic melting transition from the interdigitated to a viscous fluidlike state is observed, with an average separation distance of 2.8 nm. Cooling the sample from 70 °C causes a direct transition from the fluid into the low-temperature state with no interdigitation of the chains.

Introduction

Lipophilic fullerene (C_{60}) derivatives consist of six pairs of stearyl chains symmetrically attached around a C_{60} cage and have been shown to self-assemble within bilayers of a synthetic lecithin into rodlike structures of nanoscopic dimensions (similar to those of nanotubes). It is not yet clear whether the driving force for this self-assembly is dominated by the microelastic properties of the lipid bilayer or by the tendency of the lipo-fullerenes to form clusters. Since both the lipids and lipo-fullerenes exhibit a chain melting transition, we came to appreciate that the vast changes of molecular order and dynamics connected with it could be important for the formation of these self-assembled structures. While the phase transition behavior of lipids is well established, virtually nothing is known about the changes in structure and dynamics of the lipo-fullerenes upon the melting of its alkyl chains. Therefore, we have subjected a lipo-fullerene sample to a detailed study over a temperature range that covers the phase transition temperatures of both lipids and lipo-fullerenes (20−75 °C). We employed microcalorimetry for the detection of the transitions and combined it with solid state NMR to obtain information about molecular order and dynamics and with X-ray diffraction to resolve intermolecular correlation distances. A further motivation of this study was our finding that a bulk sample of pure lipo-fullerenes exhibits birefringence below their chain melting temperature when viewed between crossed polarizers. There is obviously a tendency of these highly symmetric molecules toward the spontaneous formation of spatially anisotropic (super)structures.

Material and Methods

The chain perdeuterated lipo-fullerene hexaadduct C_{60}−$HADC_{18}$-d_{444}, as shown in Figure 1 was obtained in three steps starting with the reduction of commercially available stearic acid-d_{35} (Fluka Chemie AG, Buchs, Switzerland) with lithium aluminum deuteride to octadecanol-d_{37} according to standard procedures. Subsequently, propanoyl dichloride was added to a cooled solution of the deuterated C_{18} alcohol in pyridine to yield dioctadecanol-d_{37} malonate (73%). The deuterated lipo-fullerene hexaadduct C_{60}−$HADC_{18}$-d_{444} was produced by cyclopropanation[1] by direct treatment of C_{60} with dioctadecanol-d_{37} malonate in the presence of dimethylanthracene, CBr_4, and diazabicycloundecene according to the literature.[2,3] The final product was characterized by ^{1}H NMR (400 MHz, $CDCl_3$) and ^{13}C NMR (100 MHz, $CDCl_3$) spectroscopy and mass spectrometry. The spectra were in agreement with the assumed structure of the reaction products; exact experimental details and spectroscopic data will be given elsewhere.[4]

The molecular mechanics calculations were carried out with the MM+ force field implanted in the program package HYPERCHEM 5.0 (Hypercube, 1995, 419 Philip Street, Waterloo, Ontario N2L3 × 2, Canada). The structure in Figure 7C was obtained after a MD simulation: During the MD simulation the structure was heated to 600 K and kept at this temperature

* Phone: 49-931-888-5863. Fax: 49-931-888-5851. E-mail: bayerl@physik.uni-wuerzburg.de.
[†] Universität Würzburg.
[‡] Universität Leipzig.
[§] University of Arizona.
[||] Universität Erlangen-Nürnberg.

10.1021/jp983427p CCC: $18.00
Published on Web 01/15/1999

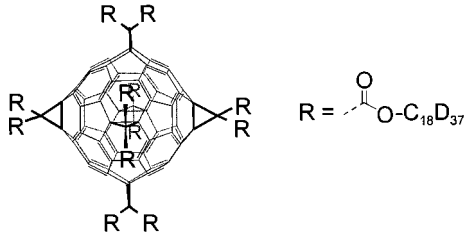

Figure 1. Schematic depiction of the lipo-fullerene C_{60}−$HADC_{18}$-d_{444}.

for equilibration before it was allowed to cool to 0 K to establish the minimum energy structure. Conditions for the simulated annealing: heat time 7 ps, run time 15 ps, cool time 25 ps, step size 1 fs, starting temperature 0 K, simulation temperature 600 K, final temperature 0 K, in vacuo.

For sample preparation, the lipo-fullerenes were dissolved in chloroform (30 mg/mL). Aliquots of the solution were pipetted either into a stainless steel sample cell (for DSC measurements), onto a glass plate (for NMR measurements), or into an X-ray capillary (for X-ray experiments), and each was dried at a pressure of 15 hPa followed by overnight (12 h) vacuum desiccation.

The DSC measurements were performed using a Hart calorimeter (Hart Scientific). Both ascending and descending temperature modes were done at a scan rate of 30 °C/h.

^{2}H NMR measurements were performed at 76.7 MHz using a Bruker AMX 500 spectrometer equipped with a Bruker broadband high-power probe having a 10 mm horizontal solenoid sample coil. The quadrupolar echo sequence with a CYCLOPS phase cycling scheme was used. The pulse spacing was 35 μs for all spectra shown, and the 90°-pulse length was 4.3−6.5 μs, depending on the probe temperature. The repetition time was 300 ms, 4096 complex data points were collected in quadrature with a dwell time of 0.4 μs, and the number of scans was 20 000 for each temperature. The temperature was controlled using the Bruker temperature control unit to within ±1 °C; for measurements below 20 °C liquid nitrogen was used as coolant.

The ^{2}H NMR spectra were obtained by setting the imaginary part of the free induction decay to zero and performing a one-dimensional Fourier transform starting at the top of the echo of the corresponding free induction decay. The first moment M_1 was calculated numerically from the corresponding spectrum $f(\omega)$ according to $M_1 = 2\int_0^\infty (\omega - \omega_0)\, f(\omega)\, d\omega / \int_{-\infty}^{\infty} f(\omega)\, d\omega$.

X-ray diffraction patterns were obtained using a pinhole camera with Ni-filtered Cu Kα radiation (30 mA/40 kV). The intensity was detected with a linear position sensitive detector system (MBraun GmbH, München, Germany). Samples were placed within a gastight, home-built diffraction cell, which was thermostated by a Julabo F10 water bath thermostat (Julabo Labortechnik GmbH, Seelbach, Germany). The 2θ range was calibrated in the range for small-angle X-ray scattering (SAXS) using the diffraction patterns of dry Ag-behenate, which exhibits a repeat distance of $d = 5.8376$ nm. For the range of wide-angle X-ray scattering (WAXS) *p*-bromobenzoic acid was used, having reflections at $d = 0.517$, 0.468, 0.380, and 0.370 nm.

Results

Thermodynamics. Differential scanning calorimetry (DSC) endotherms of C_{60}−$HADC_{18}$-d_{444} were measured in the ascending and descending temperature mode over a temperature range from −10−90 °C. An expansion of the region from 31 to 73 °C is shown in Figure 2. An endothermic transition is observed

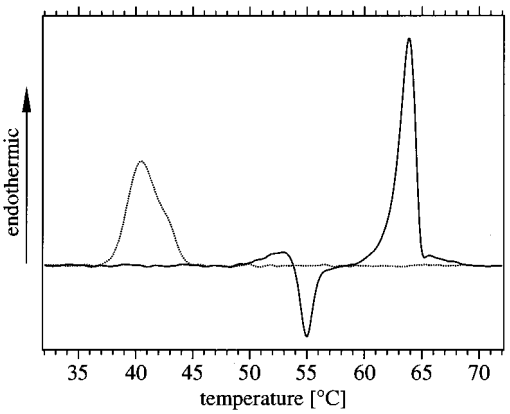

Figure 2. DSC endotherm (full line) and exotherm (dotted line) of the lipo-fullerene C_{60}−$HADC_{18}$-d_{444} at a scan rate of 30 °C/h.

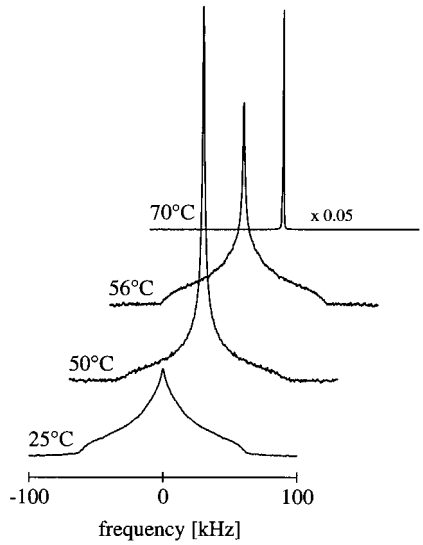

Figure 3. ^{2}H NMR spectra of the perdeuterated lipo-fullerene at 25, 50, 56, and at 70 °C (divided by 20).

at 63.8 °C (heating scan) with a full width at half-maximum (fwhm) of 1.6 °C. This transition becomes exothermic in the cooling scan and occurs at 40.5 °C (3.5 °C fwhm). The large hysteresis of 23.3 °C of this transition depends on the scan rate, which was 30 °C/h for the data shown in Figure 2. For the scan rates 15 and 60 °C/h we observed a hysteresis of 20.9 and 26.3 °C, respectively. No thermal events outside the temperature range displayed in Figure 2 were observed.

Besides this typical melting transition, we observed an exothermic peak at 55.0 °C (fwhm = 1.2 °C) for the heating scan (Figure 2), which was not observed in the cooling scan, and which did not show any significant dependence on the scan rate. This transition is preceded by a weak and rather broad endothermic feature. The sum of the enthalpies (with the corresponding sign) of all the upscan peaks corresponds to the enthalpy of the single downscan peak within an error of 7%.

Deuterium NMR. ^{2}H NMR measurements of C_{60}−$HADC_{18}$-d_{444} were performed in two temperature regimes (above and below 0 °C) in order to obtain information about the molecular orientational order and dynamics of the sample. Representative ^{2}H NMR spectra of the perdeuterated alkyl chains of C_{60}−$HADC_{18}$-d_{444} at different temperatures above 0 °C are shown in Figure 3. At the lowest temperature of this series, the spectrum shows a rather triangular line shape with spectral edges at $\nu_Q^{\pm} = \pm 63$ kHz, i.e., a maximum quadrupolar splitting of $\Delta\nu_Q = 126$ kHz, indicating partial motional averaging of the methylene

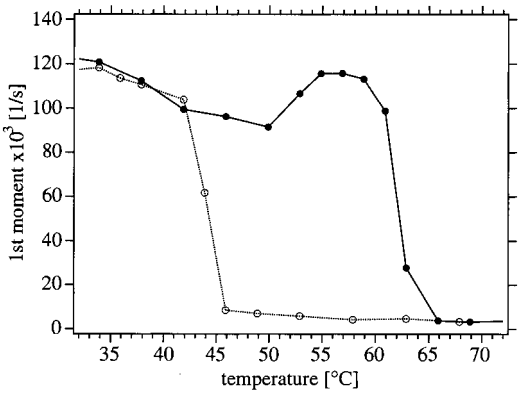

Figure 4. Plot of the first moment M_1 of ^{2}H NMR spectra as a function of temperature in the heating scan (full line) and in the cooling scan (dotted line).

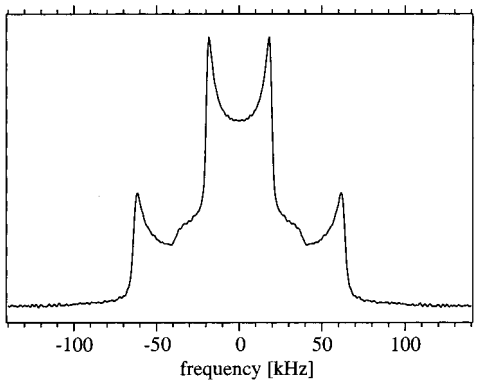

Figure 5. ^{2}H NMR spectrum of the perdeuterated lipo-fullerene at −120 °C.

deuterons (cf. Appendix). This averaging increases continuously with increasing temperature up to 50 °C, as is obvious from the growth of an isotropic signal out of the center of the spectrum and the concomitant loss of intensity at the edges of the anisotropic spectrum. Moreover, further heating of the sample from 50 to 56 °C (the region where the exothermic DSC peak was observed) causes a remarkable reduction of this isotropic signal and a corresponding increase of intensity at the spectral edges. Increasing the sample temperature further causes the isotropic signal to grow again at the expense of edge intensity. Between 60 and 65 °C there is a complete change of the anisotropic spectrum to an isotropic one, indicating complete motional averaging on the ^{2}H NMR time scale at temperatures above those where the endothermic DSC peak was observed (63.8 °C). Varying the pulse spacing in the quadrupolar echo sequence between 20 and 150 μs did not alter the shape of the spectra for any temperature.

The line shape changes with temperature can be expressed more quantitatively by calculating the first moment $M_1(T)$ of the spectra, which represents its average quadrupolar splitting, and thus is a measure of its average molecular order (Figure 4). At relatively low temperature (25 °C), the value of M_1 is similar to that observed for alkyl chains in a predominantly all-trans conformation. As the temperature is raised from 25 °C, M_1 decreases, mainly as a result of the growth of the isotropic signal. However, at 50 °C, close to the temperature of the exothermic DSC peak, M_1 starts to increase and reaches a level similar to the initial lowest temperature value at 55 °C. Concomitant to the onset of the main endothermic peak, M_1 decreases rapidly with increasing temperature, down to a level typical for alkyl chains in a fully disordered fluid state. The similarity between the moment plot and the DSC endotherms becomes even more obvious by calculating the parameter $\delta = \Delta M_1 T_m$ for 50−56 °C (giving δ_1) and for 59−65 °C (giving δ_2) and comparing the ratio δ_2/δ_1 with that of the enthalpies $\Delta H_2/\Delta H_1$ measured for both peaks by DSC. The good agreement between both ratios ($\delta_2/\delta_1 = 5.3$ and $\Delta H_2/\Delta H_1 = 4.7$) is a clear indication that M_1 provides information about the entropy of the system.

The large hysteresis observed by DSC (Figure 2) is also revealed by the NMR measurements (Figure 4). When the sample is cooled, the alkyl chains remain in a motional averaged state at temperatures well below 60 °C. At a sufficiently high level of supercooling (at 46 °C in Figure 4) the system undergoes a transition to the more ordered state characterized by a value of M_1 similar to that observed for ascending temperatures. The metastability of the fluid alkyl chains below 60 °C become obvious by supercooling the fluid sample down to 50 °C and repeatedly acquiring spectra at this temperature. Within 200 min the isotropic ^{2}H NMR line shape seen in the first spectra of this series changes to an anisotropic spectrum very similar to that shown at 50 °C in Figure 3.

Low-Temperature NMR. The line shape of the ^{2}H NMR spectrum at 25 °C shown in Figure 3 is clearly not in agreement with the theoretical expectation of a static Pake powder pattern. Some motional degrees of freedom still remain at this temperature. To understand these chain dynamics, which might be crucial for the structure and thermodynamics of the system, we have performed ^{2}H NMR measurements of this sample down to temperatures of −120 °C (Figure 5). At this temperature, the line shape is a superposition of two Pake doublets having quadrupolar frequencies of $\langle \nu_Q^{\pm} \rangle_\perp = \mp 63.5$ kHz and ± 19.5 kHz, i.e., quadrupolar splittings of 39 and 127 kHz. These splittings are expected for the methylene group of static all-trans alkyl chains, with rapid methyl group rotation about their 3-fold axis (cf. Appendix). Due to spectral distortions resulting from the finite 90°-pulse length, the relative integrated intensities of the two Pake doublets are smaller than the ratio of the number of methylene to methyl deuterons. At higher temperatures, the occurrence of gauche conformers causes an averaging of all ^{2}H NMR spectral transitions on the NMR time scale, thereby modifying the line shape more toward the triangular shape observed at 20 °C.

X-ray Scattering. To obtain information regarding positional order, we measured the correlation distances between the lipo-fullerenes at three temperatures in the ascending temperature mode. These correspond to (i) a state of the alkyl chains (25 °C) that is dominated by all-trans conformations, (ii) the state produced following the exothermic DSC peak and which is connected with the increase of M_1 (58 °C), and (iii) the disordered fluid state characterized by an isotropic ^{2}H NMR spectrum (70 °C). The results are shown in Figure 6 and listed in Table 1 and can be summarized as follows. At lowest and highest temperatures, only a single correlation distance is observed (6.1 nm at 25 °C and 2.8 nm at 70 °C), typical of a layer-like supermolecular organization. In contrast, at 58 °C two characteristic spacings (1.35 and 4.8 nm) are observed (Figure 6). The 1.35 nm peak is very weak compared to the dominant 4.8 nm peak and its higher order reflections. Their characteristic ratios in reciprocal space are a good match for a nonlamellar hexagonal arrangement of amphiphiles,[5] thus showing a distinct anisotropy in the spatial arrangement of the lipo-fullerenes. The widths of all the scattering peaks (fwhm 0.24−0.28 °2θ) except that at 70 °C indicate spatial correlation lengths of about 4−6 times the corresponding distances.

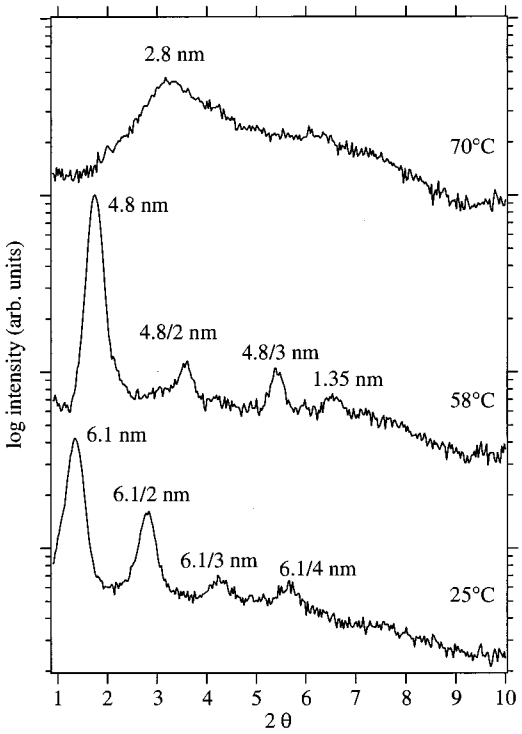

Figure 6. X-ray diffraction patterns of the lipo-fullerene C_{60}−$HADC_{18}$-d_{444}, measured at three temperatures: 25 °C (top), 58 °C (middle), and 70 °C (bottom). The correlation distances corresponding to the dominant peaks are given.

TABLE 1: Characteristic Lengths Derived from the Diffraction Patterns of the Lipo-Fullerene C_{60}-$HADC_{18}$-d_{444} (Figure 6) for the Three Temperature Ranges Measured by X-ray Diffraction

temp (°C)	distance (nm)
25	6.1 ± 0.1
58	$1.35 \pm 0.2/4.80 \pm 0.1$
70	2.8 ± 0.2

Discussion

The combination of results from differential scanning calorimetry, deuterium NMR spectroscopy, and X-ray diffraction allows a consistent interpretation of the thermotropic behavior of lipo-fullerenes in terms of a structural model, which includes the essential dynamical features of these molecules. The present work suggests that three structurally different states of the bulk lipo-fullerenes can be distinguished, which are depicted in a structural model shown in Figure 7.

1. Below 50 °C, the 12 alkyl chains of each lipo-fullerene are stiff and become increasingly all-trans with decreasing temperature, thereby pointing away on average from the fullerene cage in a radial direction. The theoretical expectation of the lipo-fullerene diameter d_1 is then the sum over twice the all-trans length of a C18 alkyl chain plus the C_{60} diameter; thus $= (2 \times 2.3 + 1.2)$ nm $= 5.8$ nm. In contrast, the largest MM+ calculated diameter (cf. Methods) of the lipo-fullerene with the lowest energy all-trans conformation of the alkyl chains is 5.6 nm. The 0.2 nm discrepancy results from the consideration of the slight deviation of the alkyl chains from the radial direction (Figure 7A) indicated by the MM+ calculation. Both values are close to the correlation distance of 6.1 ± 0.2 nm measured for this state (Table 1), so that one can assume distorted cubic packing and intercalation (interdigitation) between the chains of adjacent molecules is very unlikely. The discrepancy of 0.3 nm between the theoretical expectation and experiment is probably a result of the residual intramolecular chain dynamics, which hampers closest packing and thus keeps the correlation length of the 3-dimensional arrangement larger than otherwise. The temporal occurrence of gauche conformers along with the above-mentioned rotation of the chain segments, as evident from the ^{2}H NMR results, is a likely reason for this (dynamic) packing defect. Since the free volume increases toward the end of the chain and is largest in the region of the terminal methyl group, this region exhibits the highest probability of gauche states. The almost linear reduction of M_1 from 20 to 50 °C is most likely caused by an increase of gauche states predominantly in this

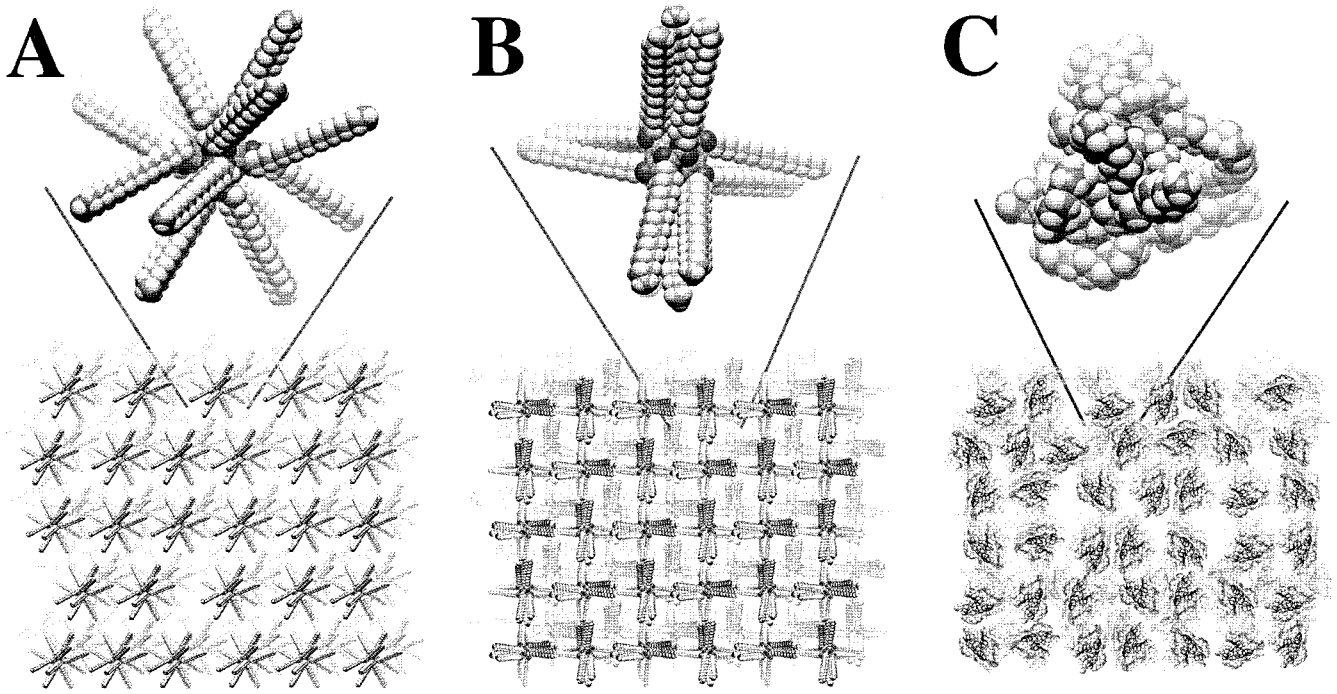

Figure 7. Schematic depiction of the suggested arrangement of the lipo-fullerenes for the three temperature ranges upon heating the sample (not to scale): (A) the low-temperature state existing below 50 °C; (B) the interdigitated state existing between 55 and 68 °C; (C) the fluidlike state existing above 70 °C. For cooling the sample, the interdigitated state is omitted.

region of largest free volumes. On the contrary, as the probability of gauche states becomes very low at temperatures of −120 °C, M_1 is very large and the packing can be expected to approach closest packing at this temperature.

2. At temperatures above 50 °C the probability of gauche conformer formation at chain positions close to the C_{60} cage reaches a sufficiently high level to allow the chains to tilt with respect to each other, thereby forming bunches of more or less parallel chains and reducing the symmetry. This formation of bunches may consume some energy, but it gives rise to a significantly denser packing by mutual penetration of bunches into the "hard sphere" diameter of adjacent molecules (interdigitation). The driving force for this process is the optimization of strong van der Waals interactions between the chains, which is hampered by the stiffness of the chains leading to a "hard sphere packing" at temperatures below 50 °C. The weak endothermic signal preceding the exothermic peak at 55 °C in Figure 2 might indicate that local melting of the chains is a prerequisite for the interdigitation occurring at 55 °C. The large energy gain through the interdigitation-optimized van der Waals interaction, and the concomitant reduction of free volume between the chains due to interdigitation of adjacent molecules manifests itself by the exothermic DSC peak (Figure 2) at this temperature. This is accompanied by the observed reduction of the isotropic component in the ^{2}H NMR spectrum at 56 °C (Figure 3) and the increase of the first moment (Figure 4). The correlation distance between adjacent C_{60} cages becomes 4.8 nm after interdigitation and thus is 1.3 nm closer than under low-temperature conditions. This indicates a mutual penetration between the chains down to about the 12th carbon of each chain, resulting in close packing of the lipo-fullerenes in a quasi two-dimensional hexagonal lattice. The increase of M_1 suggests an increase of molecular order. This is indeed expected because of the significant reduction of gauche conformer probability in the interdigitated region by the reduction of free volume. Note that the interdigitation reduces the motional freedom particularly for those segments (methylenes close to the terminal methyl group) that are most prone to the formation of gauche states at temperatures below 50 °C.

3. Above the chain melting transition at 63.8 °C the disorder of the alkyl chains becomes the dominant feature, which causes an abrupt drop of M_1 and a further reduction of the correlation distance between the C_{60} cages down to 2.8 nm at 70 °C. The significantly increased full width at half-maximum of the X-ray peak (Figure 6) indicates a drop in spatial correlation distance. We interpret this state as quasi-fluid alkyl chains surrounding each rigid C_{60} cage, keeping them at a minimum distance from each other by a cushion of steric repulsion between the fluid chains "grafted" symmetrically to the cages. Nevertheless, there are significant differences from real fluids. Although any short-range order seems to be lost in this state, as indicated by the isotropic ^{2}H NMR spectrum, some long-range order is still left, giving rise to the broad X-ray signal. There seems to be some tendency of the now completely symmetric molecules to keep a "next neighbor" ordering in this state, similar to a distorted cubic packing under viscous-fluid conditions.

One should note that the above three-state model is applicable only for the states produced on heating the sample. Both the DSC and ^{2}H NMR results indicate that, by cooling the sample, the interdigitated state is omitted, and the lipo-fullerenes undergo a transition directly into the low-temperature state. The large hysteresis can be understood by the strong attractive van der Waals interaction between the fluid chains and the C_{60} cages immersed in between. The formation of all-trans chains during the cooling requires first an increase of the correlation distance between the adjacent C_{60} moieties against this attractive force. This requires substantial undercooling until the lifetime of the formed trans conformations becomes sufficiently long to force the molecules apart.

It is interesting to note that the observed interdigitated state does not exist when the lipo-fullerenes are forced to accommodate a spatial geometry, which is different from their bulk properties, as in the case of their intercalation into phospholipid bilayers.[6] Here the self-assembly of quasi two-dimensional structures seems to prevent interdigitation, and by contrast only the chain melting transition is observed. As a result, the system is transformed directly from the ordered low-temperature state to the disordered fluid state.

Conclusion

The lipophilic derivatized C_{60} studied in this work exhibits a thermotropic phase behavior, which can be described by a three-state model. An interdigitated state is observed upon heating the sample, which is intermediate between the states at low and high temperature. Future studies can concentrate on the question of whether these transitions are connected with changes of optical properties such as birefringence.

Acknowledgment. This work was supported by a grant from the Deutsche Forschungsgemeinschaft; the work of M.F.B. was sponsored by the U.S. National Institutes of Health.

Appendix 1: Effect of Intramolecular Motion on the ^{2}H NMR Line Shape

We shall assume that the static electrostatic field gradient (EFG) tensor in the case of an aliphatic C−^{2}H bond is axially symmetric about the bond axis, with coupling parameters of $\chi_Q = e^2qQ/h = 170$ kHz and the asymmetry parameter $\eta_Q = 0$. The quadrupolar frequencies are then given by

$$\nu_Q^{\pm} = \pm \frac{3}{4}\chi_Q D_{00}^{(2)}(\Omega_{PL}) = \pm \chi_Q\left(\frac{3\cos^2\beta_{PL} - 1}{2}\right) \quad (1)$$

The above expression describes the dependence of the quadrupolar splitting on the (Euler) angles $\Omega_{PL}(\alpha_{PL},\beta_{PL},\gamma_{PL})$ that transform the coupling tensor from its principal axis system (PAS) P to the laboratory frame L, defined by the main magnetic field.

In the present case powder-type samples are studied, which give rise to singularities and discontinuities in the spectral intensity distribution. For the case of a static polymethylene chain, the discontinuities correspond to eigenfrequencies that are given by $(\nu_Q^{\pm})_{\perp} = \mp 3\chi_Q/8 = \mp 63.75$ kHz and $(\nu_Q^{\pm})_{\parallel} = \pm 3\chi_Q/4 = \pm 127.5$ kHz, respectively, yielding a total spectral breadth of 255 kHz.

Motion of the hydrocarbon chains changes the static coupling tensor to an effective tensor described by the parameters χ_Q^{eff}, which are reduced in magnitude by the motional averaging.[7,8] This can be described in an irreducible tensor representation, which simplifies the treatment of multiple motions,[9] and the following limiting motional cases can be considered.

(i) For a motion of relatively low symmetry, like two-site jumps of a C^2H_2 group (equally probable sites) of a nonrotating polymethylene chain on a diamond lattice, one obtains $\langle V_{xx}\rangle = 0$ kHz in the laboratory frame. The other two components are easily calculated in a Cartesian basis[10] to yield $\langle V_{zz}\rangle = \mp 3\chi_Q/8 = \mp 63.75$ kHz and $\langle V_{yy}\rangle = \pm 3\chi_Q/8 = \pm 63.75$ kHz. Here V_{xx},

V_{yy}, and V_{zz} are the diagonal elements of the EFG in the principal axis system. Consequently, one obtains a powder pattern having discontinuities at (−63.75, 0, +63.75) kHz, and a total spectral breadth of 127.5 kHz.

(ii) For the case of 3-fold or higher rotational symmetry like an all-trans polymethylene chain undergoing rotation about its long axis, the singularities occur at $\langle \nu_Q^{\pm} \rangle_\perp = \mp 3\chi_Q/8 = \mp 63.75$ kHz and $\langle \nu_Q^{\pm} \rangle_{||} = \pm 3\chi_Q/16 = \pm 31.875$ kHz. Here the angular brackets denote the averaging due to axial rotations that are fast on the NMR time scale (5×10^{-6} s for deuterium NMR).

(iii) Likewise, various motions of the terminal C^2H_3 groups of a polymethylene chain can be treated. For rotation about the 3-fold axis of a methyl group bonded to an otherwise rigid polymethylene chain, one obtains values of $\langle \nu_Q^{\pm} \rangle_\perp = \pm\chi_Q/8 = \pm 21.25$ kHz and $\langle \nu_Q^{\pm} \rangle_{||} = \mp\chi_Q/4 = \mp 42.5$ kHz for the perpendicular and parallel components, respectively, having a total width of 85.0 kHz. If, in addition to the 3-fold methyl rotation, the polymethylene chain itself undergoes long axis rotation, then discontinuities result at $\langle \nu_Q^{\pm} \rangle_\perp = \pm\chi_Q/16 = \pm 10.625$ kHz and $\langle \nu_Q^{\pm} \rangle_{||} = \mp\chi_Q/8 = \mp 21.25$ kHz, with a total breadth of 42.5 kHz.

References and Notes

(1) Bingel, C. *Chem. Ber.* **1993**, *126*, 1957.

(2) Lamparth, I.; Maichle-Moessmer, C.; Hirsch, A. *Angew. Chem.* **1995**, *1078*, 1755−1757.

(3) Camps, X.; Hirsch, A. *J. Chem. Soc., Perkins Trans 1* **1997**, 1595.

(4) Camps, X. Manuscript in preparation.

(5) Seddon, J. *Biochim. Biophys. Acta* **1990**, *1031*, 1−69.

(6) Hetzer, M.; Bayerl, S.; Camps, X.; Vostrowsky, O.; Hirsch, A.; Bayerl, M. T. *Adv. Mater.* **1997**, *9*, 913−917.

(7) Brown, M. F.; Söderman, O. *Chem. Phys. Lett.* **1990**, *167*, 158−164.

(8) Trouard, T. P.; Alam, T. M.; Zajicek, J.; Brown, M. F. *Chem. Phys. Lett.* **1992**, *189*, 67−75.

(9) Brown, M. F. Membrane structure and dynamics studied with NMR spectroscopy. In *Biological membranes. A molecular perspective from computation and experiment*; Merz, J. K., Roux, B., Eds.; Birkhäuser: Basel, 1996; pp 175−252.

(10) Huang, T. H.; Skarjune, R. P.; Wittebort, R. J.; Griffin, R. G.; Oldfield, E. *J. Am. Chem. Soc.* **1980**, *102*, 7377−7379.